Volume 54
Number 39
21 October 2025
Pages 14599-14978

Dalton Transactions

An international journal of inorganic chemistry

rsc.li/dalton

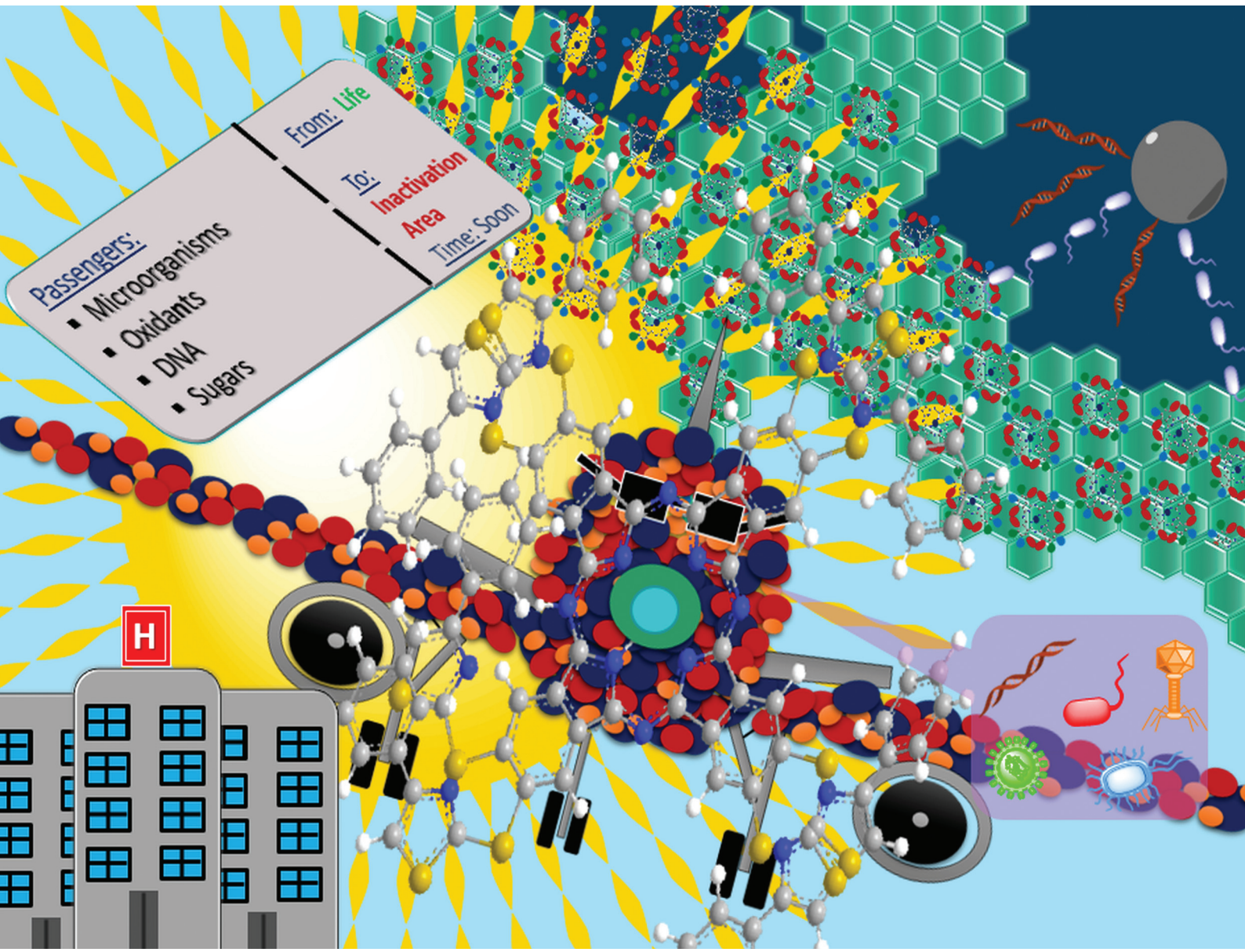

ISSN 1477-9226

ROYAL SOCIETY OF CHEMISTRY

PAPER

Nazli Farajzadeh Öztürk *et al.*

Biological activities of metallic nanostructures functionalized with hexadeca-substituted copper(II) and cobalt(II) phthalocyanines

Dalton Transactions

ROYAL SOCIETY OF CHEMISTRY

PAPER

View Article Online
View Journal | View Issue

Cite this: *Dalton Trans.*, 2025, **54**, 14664

Biological activities of metallic nanostructures functionalized with hexadeca-substituted copper(II) and cobalt(II) phthalocyanines

Nazli Farajzadeh Öztürk, *[a] Sadin Özdemir,[b] M. Serkan Yalçın,[c] Zehra Altuntaş Bayır *[d] and Makbule Burkut Koçak *[d]

A novel phthalonitrile derivative (**a**) containing three functional groups (hexyl, aminated ester, phenoxy) was synthesized and subsequently cyclotetramerized in the presence of the corresponding metal chloride salts to obtain hexadeca-substituted metal {M = Cu(II) and Co(II)} phthalocyanines (**b** and **c**). The water-soluble phthalocyanines (**d** and **e**) were prepared by treating the newly synthesized complexes (**b** and **c**) with methyl iodide. Moreover, gold nanoparticles (**1**) and silver nanoparticles (**2**) were prepared, and their surfaces were modified with quaternary phthalocyanines (**d** and **e**). The biological properties of both unmodified (**1** and **2**) and functionalized nanostructures (**1d**, **1e**, **2d**, and **2e**) were extensively studied. All nanomaterials exhibited moderate antioxidant activity. Nanoconjugate (**2e**) at 100 mg L^{-1} displayed the highest inhibitory activity (98.7%) against α-amylase. Moreover, all nanostructures cleaved DNA molecules at 100 mg L^{-1}. The MIC of nanostructures (**1**, **2**, **1d**, **1e**, **2d**, and **2e**) ranged from 2 to 64 mg L^{-1} for inhibiting bacterial growth. Additionally, all nanostructures (especially modified silver nanostructures) demonstrated greater biofilm inhibition activity against *S. aureus* compared with *P. aeruginosa*. Surficial modification of nanostructures with resultant phthalocyanines improved their microbial cell viability inhibition activity against *E. coli*, particularly after irradiation. This significant improvement in the biological activities of metallic nanoparticles suggests that, with further investigation, these new nanoconjugates could be considered promising candidates for medical nanomaterials.

Received 26th May 2025,
Accepted 23rd August 2025

DOI: 10.1039/d5dt01232e

rsc.li/dalton

Introduction

The lack of effective drugs for the prevention or treatment of serious disorders (*e.g.*, cancer, diabetes, and infections) that can lead to fatal outcomes is considered one of the essential global concerns. Fluorine chemistry is well-known as a multidisciplinary interface between biology and chemistry, owing to its vital role in cancer biology, chemical biology, medicinal chemistry, and molecular imaging. The presence of fluorine in organic systems can improve their electronic properties, chemical stability, selective reactivity, and solubility because the addition of highly electronegative fluorine atoms alters electron distribution, resulting in a highly polarized C–F bond.[1] Additionally, fluorine can modify the bioavailability, lipophilicity, protein binding affinity, and metabolic reactivity of organic molecules[2,3] by refining molecular conformation, acidity/basicity, intrinsic potency, and membrane permeability.[4] Recently, fluorine-containing materials have been considered suitable pharmaceutical alternatives for many types of medicines, including antibiotics, antidepressants, anesthetics, antiviral, anti-cancer, psychotropic, and biocompatible agents.[5]

The biodegradability of esters leads to their limited accumulation in the environment.[6] Additionally, the degradation of ester-containing materials in soil and water generally results in comparatively friendly degradative byproducts to nontarget organisms and the environment.[7] Many studies have reported the fungicidal activities of ester-containing compounds. Although benzyl alcohols can improve the fungicidal activity or broaden the spectrum of esters, the fusion of different heterocyclic groups to the benzene ring often reduces their bioactivities.[8,9] Therefore, the design of a strategic procedure for the preparation of biologically active benzyl ester-containing materials using the acidic proton of the esters is a key research area for scientists.

Amines are functional organic systems bearing a nitrogen atom with one lone pair. Due to their ease of synthesis and relative stability, the preparation of aminated derivatives has

[a]*Department of Analytical Chemistry, Faculty of Pharmacy, Acıbadem Mehmet Ali Aydınlar University, Ataşehir, Istanbul, 34752, Türkiye.*
E-mail: nazli.ozturk@acibadem.edu.tr
[b]*Food Processing Programme, Technical Science Vocational School, Mersin University, TR-33343 Yenişehir, Mersin, Türkiye*
[c]*Department of Chemistry and Chemical Processing Technologies, Technical Science Vocational School, Mersin University, 33343, Mersin, Türkiye*
[d]*Department of Chemistry, Istanbul Technical University, Maslak, Istanbul, 34469, Türkiye. E-mail: bayir@itu.edu.tr, mkocak@itu.edu.tr*

been of interest in pharmaceutical and combinatorial chemistry.[10–13] These compounds are the main components of many structures, such as adhesives, cosmetics, drugs, dyes, pesticides, polymers, and solvents.[14,15] In addition, N-containing macrocycles encompassing chlorins, corroles, porphyrins, and phthalocyanines are highly fascinating compounds in many scientific and high-technological fields.[16]

Four indole units assemble to form a phthalocyanine ring, which can accommodate diverse metal cation(s) in the core and bulky organic groups at the periphery.[17] Indeed, the specific architectural structure of phthalocyanine rings leads to the easy systemic modification that in turn dedicates unique chemical, electrical, and physical features to the phthalocyanines.[18–20] Therefore, the conscious alteration of the phthalocyanine rings can be a suitable alternative to designing efficient materials for science and technology.[21–30] In particular, the presence of fluorine atoms in their structures can refine biochemical potency, including lipophilicity, photostability, selective accumulation, and singlet oxygen generation.[31,32] The possibility of the modification of nanomaterials has been of interest in recent years, but there is a huge vacancy in this research field. Functionalization of nanomaterials with different inorganic/organic molecules such as peptides, polymers, and biomolecules suggests the capability to conjugate multiple therapeutic agents or biomacromolecules covalently or non-covalently, and can lead to desired properties like specific recognition or biocompatibility.[33,34] Additionally, the biological effect of cobalt and copper complexes on bioreductive activation, protein inhibition, and drug activity has attracted attention in recent decades.[35,36] Our research team has focused on the design of phthalocyanine-functionalized nanostructures and the study of the role of phthalocyanines on the functional properties of nanomaterials.[37–43]

"Nanomaterials" are defined as materials with at least one dimension ≤100 nm. Nanostructures have a high surface/volume area ratio, outstanding quantum-size effect, and excellent surface chemistry. Therefore, they exhibit amazing chemical and physical features that are not observed in their bulk counterparts. Additionally, these unique properties extensively affect their applications in many fields, ranging from engineering to medicine.[44,45] Based on composition, nanosized materials are categorized into four major groups of nanostructure: inorganic, organic, carbon-based, and composite-based. Inorganic nanomaterials contain at least one type of metal atom in their structures, and include metal, metal oxides, and magnetic nanostructures in various sizes and shapes. In addition, metallic nanoclusters, nanoclays, zeolites, and MXenes are devoted to this group. Metal nanoparticles display excellent chemical, biological, electrical, catalytic, and optical features.[46–48] In particular, the greater surface-to-volume ratio of metal nanostructures leads to biotic responses owing to unique properties not observed in their bulk forms. Moreover, their surface can be readily modified by diverse compounds such as antibodies, biomolecules, DNAs, drugs, ligands, peptides, and targeting agents as well as polymers.[49–52] However, few studies have presented the surficial functionalization of metal nanostructures with phthalocyanines, and most studies have been reported by our research team.[37–44]

The increasing utility of nanomaterials in a wide range of scientific and technological applications has led to their significant exposure to the environment and humans. Generally, nanoparticles with a small range of sizes have exhibited few toxic effects on mammalian cells.[53,54] Facile synthesis, tunable sizes, strong optical features, and easy modification make gold nanoparticles suitable agents for biomedical applications.[55] Although there is some uncertainty about the toxicity of gold nanoparticles, some reports have indicated non-significant toxicity for these biocompatible materials.[56–59] Nelson *et al.* revealed that citrate-capped gold nanoparticles do not result in discrete cell death, oxidative damage to DNA, or the production of free radicals.[58] Due to antibacterial, antiviral, and antifungal activities, silver nanoparticles have been of interest in biomedical fields such as biomedical sensing, molecular imaging, drug delivery, and cancer therapy.[60–63] Mulenos *et al.* reported that the production of silver ions contributes to toxicity, and that controlling their generation reduces toxicity (6.9 μg mL^{-1} under oxic conditions and 0.2 μg mL^{-1} under anoxic conditions).[64]

Generally, microbes are classified into two categories: eukaryotes and prokaryotes. Eukaryotes have a cell nucleus in their structure and consist of a vast range of microorganisms such as algae, protists, and fungi.[65] Bacteria and related archaea are included in prokaryotes whose genetic materials are not surrounded by a membrane (nuclear envelope). Pathogenic microbes are responsible for infectious diseases because they invade the host and obtain nutrition from it. An individual or population of pathogenic microbes can invade and proliferate rapidly within the host body. An infection may not always induce a disease, but any damage to the vital functions of the body results in illness. Being pathogenic, diverse bacteria, fungi, nematodes, and viruses infect animals and plants. Infectious diseases are fundamental threats to humans and ecosystems worldwide. Efficient pretreatment and treatment of infections require precise and rapid diagnosis of at-risk or infected individuals through the application of simple and low-cost methods or materials.[66,67] Several studies revealed the high antimicrobial activities of metal phthalocyanines and metal nanostructures.[68–71]

Meanwhile, free radicals are highly reactive and unstable, which enables them to participate in chemical reactions with a wide range of molecules. Unfortunately, such reactions can result in unavoidable damage that can impair several repair processes.[72] Free radicals are atoms, ions, and molecules that contain unpaired electrons and are typically derived from nitrogen, oxygen, or sulfur. Reactive oxygen species (ROS) are oxygen-centered free radicals such as alkoxyl ($RO^{\bullet}$), hydroxyl ($HO^{\bullet}$), nitric oxide ($NO^{\bullet}$), peroxyl ($ROO^{\bullet}$), and superoxide ($O_2^{\bullet-}$). Although they usually exist as byproducts of normal metabolism in cells, they can damage carbohydrates, lipids, nucleic acids, and proteins.[73] Antioxidants play a vital role in maintaining the normal function and viability of living cells. Hence, in recent years, researchers have shown increasing

interest in the antioxidant potency of materials (especially phthalocyanines and nanomaterials) to discover or design efficient antioxidant agents.

Few scholars have reported the synthesis and characterization of heterocycle-containing nanomaterials for biological applications. However, the synthesis and characterization of hexadeca-substituted phthalocyanines require more effort. The synthesis and biomedical features of nanoparticles modified with hexadeca-substituted phthalocyanines have not been reported, to the best of our knowledge. Herein, we present the synthesis of a new tetra-substituted phthalonitrile derivative and its hexadeca-substituted metal phthalocyanines. The resulting metal complexes, bearing three groups (amine-ester, fluorinated, and long alkyl substituents), were treated with methyl iodide to make them water-soluble. Then, they were used for the surficial modification of two prepared metallic nanostructures: gold and silver nanoparticles. Additionally, the biological properties (antioxidant, antidiabetic, DNA cleavage, antimicrobial, and antibiofilm activities) of the resultant nanoconjugates were extensively examined to assess the synergistic effect of metal ions/atoms upon bioactivity. Hence, our study provides insights into effective heterocycle-based nanomaterials for multidisciplinary biological applications.

Experimental

Synthesis and characterization

Diethyl 2-(3,4-dicyano-2,5-bis(hexyloxy)-6-(4-(trifluoromethoxy) phenoxy)phenyl)malonate was synthesized according to a procedure described extensively in ref. 43.

Potassium salt of diethyl 2-(3,4-dicyano-2,5-bis(hexyloxy)-6-(4-(trifluoromethoxy)phenoxy)phenyl) malonate

Diethyl 2-(3,4-dicyano-2,5-bis(hexyloxy)-6-(4-(trifluoromethoxy) phenoxy)phenyl) malonate (1 g, 1.51 mmol) was dissolved in ethanol at reflux temperature. After the addition of potassium hydroxide (0.337, 6.04 mmol) to the mixture, the potassium salt was precipitated and washed several times with cold ethanol.[74] Yield: 0.920 g (%87). FT-IR ν (cm^{-1}): 3070 (aromatic CH), 2958 (aliphatic CH), 2223 (C≡N), 1728 (C=O), 1100 (C–O–C).

Diethyl 2-(3,4-dicyano-2,5-bis(hexyloxy)-6-(4-(trifluoromethoxy) phenoxy)phenyl)-2-(2-(dimethylamino)ethyl)malonate (a)

The potassium salt of diethyl 2-(3,4-dicyano-2,5-bis(hexyloxy)-6-(4-(trifluoromethoxy)phenoxy)phenyl) malonate (1 g, 1.43 mmol) and 2-chloro-*N*,*N*-dimethylethylamine (0.768 g, 7.13 mmol) were dissolved in acetonitrile and stirred for 72 h at 80 °C. After solvent evaporation, the solid product was crystallized from ethanol.[74] Chemical formula: $C_{38}H_{50}F_3N_3O_8$. Yield: 0.660 g (%63). FT-IR ν (cm^{-1}): 3067 (aromatic CH), 2959 (aliphatic CH), 2207 (C≡N), 1711 (C=O), 1091 (C–O–C). ^{1}H NMR (500 MHz; DMSO-d_6): δ (ppm) 7.27–7.24 (d, 2H), 7.01–6.98 (d, 2H), 3.98–3.92 (m, 4H), 3.87–3.83 (m, 4H), 3.17–3.14 (m, 4H), 2.53 (s, 6H), 1.58–1.54 (m, 4H), 1.31–1.27 (m, 12H), 0.94–0.91 (m, 6H), 0.88–0.85 (t, 6H).

General procedure for the synthesis of metal phthalocyanines

Compound **a** (0.100 g, 0.136 mmol) and the related anhydrous metal salts {$CuCl_2$ (0.005 g, 0.034 mmol); $CoCl_2$ (0.005 g, 0.034 mmol)} and 1,8 diazabisiklo[5.4.0]undek-7-en (DBU) were stirred in *n*-pentanol at 150 °C for 24 h. During the cyclotetramerization of compound **a**, transesterfication occurred, leading to the replacement of ethyl groups with the pentyl groups from the solvent.[42] The reaction mixture was poured into a 2 : 1 mixture of water and ethanol, stirred for 1 h, and filtered off. The precipitate was purified using a chromatographic method on silica gel as a stationary phase and a mixture of dichloromethane : *n*-hexane (1 : 1) as a mobile phase.

CuPc (b). Yield: 0.037 g (%32.5), m.p. > 250 °C. FT-IR ν (cm^{-1}): 3061 (aromatic CH), 2960 (aliphatic CH), 1725 (C=O), 1084 (C–O–C). UV–vis (DMSO): λ_{max} nm ($\log \varepsilon$) 388 (4.89), 712 (5.23). MS (MALDI-TOF): *m*/*z* calc. $[M]^+$ 3335.50 found 3337.01 $[M + 2H]^+$, 3289.66 $[M - Cu + H_2O]^+$. Anal. calcd for $C_{176}H_{248}CuF_{12}N_{12}O_{32}$ C, 63.38; H, 7.49; N, 5.04 found: C 64.02, H 7.78, N 5.15%.

CoPc (c). Yield: 0.032 g (%28), m.p. > 250 °C. FT-IR ν (cm^{-1}): 3070 (aromatic CH), 2962 (aliphatic CH), 1725 (C=O), 1080 (C–O–C). UV–vis (DMSO): λ_{max} nm ($\log \varepsilon$) 381 (5.14), 710 (5.33). MS (MALDI-TOF): *m*/*z* calc. $[M]^+$ 3330.89 found 3330.91 $[M]^+$; 2835.91 $[M - 3C_7H_4F_3O_2 + 2H_2O]^+$. Anal. calcd for $C_{176}H_{248}CoF_{12}N_{12}O_{32}$ C, 63.46; H, 7.50; N, 5.05% found: C 64.80, H 7.83, N 5.13%.

Water-soluble metal phthalocyanines

First, 0.050 g of each macromolecule (**b** or **c**; 0.015 mmol) and iodomethane (0.009 g, 0.060 mmol) were dissolved in chloroform (5 mL) and stirred at room temperature for 72 h. The reaction content was filtered off, washed several times with chloroform, and dried.

QCuPc (d). Yield: 0.044 g (%75), m.p. > 250 °C. FT-IR ν (cm^{-1}): 3070 (aromatic CH), 2957 (aliphatic CH), 1727 (C=O), 1096 (C–O–C). UV–vis (DMSO): λ_{max} nm ($\log \varepsilon$) 378 (5.30), 706 (4.95). MS (MALDI-TOF): *m*/*z* calcd $[M]^+$ 3903.26 found 3522.05 $[M - 3I]^+$; 3288.20 $[M - I - 3C_7H_4F_3O_2 + Na + H_2O + 2H]^+$ 3061.86 $[M - 4I - 2C_7H_4F_3O_2 + 2H + H_2O]^+$.

QCoPc (e). Yield: 0.047 g (%80), m.p. > 250 °C. FT-IR ν (cm^{-1}): 3066 (aromatic CH), 2941 (aliphatic CH), 1721 (C=O), 1101 (C–O–C). UV–vis (DMSO): λ_{max} nm ($\log \varepsilon$) 372 (5.07), 705 (4.76). MS (MALDI-TOF): *m*/*z* calc. $[M]^+$ 3898.64 found 3644.07 $[M - 2I]^+$, 3487.01 $[M - 3I - 2CH_3]^+$.

Gold nanoparticles (1)

First, 100 mL of an aqueous solution of hydrogentetrachloroaurate (1% w/v) was heated to boiling. After the addition of trisodium citrate solution (1% w/v, 5 mL), the mixture changed from yellow to red. The obtained suspension of gold nanoparticles was cooled to room temperature and stored at 4 °C.[41] The concentration of diluted nanoparticles (**1**) was ~50 μg mL^{-1}.

Silver nanoparticles (2)

First, 220 mL of an aqueous solution containing $AgNO_3$ (1 mM) and trisodium citrate (3 mM) was stirred vigorously under an inert atmosphere. Then, 20 μL of $NaBH_4$ solution

(0.2 M) was added to the reaction content. The mixture turned yellow after 15 min. The suspension was refrigerated.[75] The concentration of diluted nanoparticles (**2**) was ~50 μg mL^{-1}.

Preparation of nanoconjugates (1d, 1e, 2d, and 2e)

The surface of the metallic nanostructures was modified by compounds (**d** and **e**) according to the method explained in ref. 37,41 with some modifications. Initially, 10 mg of each compound (**d** or **e**) was dissolved in 1.1 mL of a DMF/distilled water (1/100 v/v) and added to 9 mL of concentrated metallic nanoparticles (**1** or **2**). The solution was stirred for 24 h at room temperature.[37,41] The nanoconjugates were filtered off, collected, and dispersed in distilled water. The same procedure was applied for the preparation of modified silver nanoparticles (**2d**, and **2e**).

Biological studies

For biological experiments, the test compounds were dissolved in dimethyl sulfoxide (DMSO). Each biological test was done in three replicates.

Antioxidant activity

The 2,2-diphenyl-1-picrylhydrazyl (DPPH) free radical-scavenging assay was applied to evaluate the antioxidant potency of the prepared unmodified (**1** and **2**) and modified nanostructures (**1d**, **1e**, **2d**, and **2e**). Different concentrations (6.25–100 mg L^{-1}) of each nanomaterial (**1**, **2**, **1d**, **1e**, **2d**, or **2e**) were mixed with DPPH (0.002%) in methanol and stirred vigorously. The absorbance was determined at 517 nm after a 0.5 h incubation at 25 °C in the dark. Ascorbic acid and Trolox were utilized as positive controls. In addition, a sample of reagents without nanomaterials (**1**, **2**, **1d**, **1e**, **2d**, or **2e**) was used as a negative control. The free radical-scavenging activity was calculated using eqn (1).

$$\text{DPPH Inhibition}\,(\%) = \left(\frac{\text{Abs}_{\text{control}} - \text{Abs}_{\text{sample}}}{\text{Abs}_{\text{control}}}\right) \times 100 \quad (1)$$

Antidiabetic activity

Different concentrations (25, 50, and 100 mg L^{-1}) of each nanomaterial (**1**, **2**, **1d**, **1e**, **2d**, or **2e**), α-amylase, and phosphate buffer were added to test tubes and kept at 37 °C for 15 min. Hydrolysis occurred upon the addition of 0.2 mL of a 1% potato starch solution. After 20 min incubation at 37 °C, 400 mL of 3,5-dinitro salicylic acid (DNS) was added to the test tubes to suppress the hydrolysis and then kept in boiling water for 5 min. After cooling to room temperature, the mixture was diluted by adding distilled water (3 mL). The absorbance was measured at 540 nm. A solution without nanostructures was used as a control. The antidiabetic activities of nanomaterials (**1**, **2**, **1d**, **1e**, **2d**, and **2e**) was determined by applying eqn (2).

$$\text{Antidiabetic activity}\,(\%) = (\text{Control}_{\text{abs}} - \text{Sample}_{\text{abs}})/\text{Control}_{\text{abs}} \times 100 \quad (2)$$

DNA cleavage activity

First, 15 μL of each nanomaterial (**1**, **2**, **1d**, **1e**, **2d**, or **2e**) and pBR322 plasmid DNA (5 μL) were added to a PCR tube and incubated at 37 °C for 2 h in the dark at 50, 100 and 200 mg L^{-1}. A 1% agarose gel was placed in an electrophoresis tank and fixed. Then, the tank was filled with Tris-acetate-EDTA buffer until the gel was completely covered. Each prepared sample was loaded into a gel well after the addition of loading dye. Electrophoresis was conducted at 100 V for 1 h. The gel was carefully removed from the electrophoresis tank and observed using a UV transilluminator.

Antimicrobial activity

A microdilution method was applied to examine the antimicrobial properties of nanomaterials (**1**, **2**, **1d**, **1e**, **2d**, and **2e**) against some microorganisms: *Enterococcus hirae* (ATCC 10541), *Escherichia coli* (ATCC 10536), *Staphylococcus aureus* (ATCC 6538), *Bacillus cereus*, *Legionella pneumophila* subsp. *pneumophila* (ATCC 33152), *Pseudomonas aeruginosa* (ATCC 9027), *Candida parapsilosis*, and *Candida tropicalis*. Fresh cultures were cultivated for 24 h before implementation. Prepared samples were serially diluted twice in 96-well plates from 1024 mg L^{-1} to 1 mg L^{-1} and incubated for 24 h at 37 °C. Then, the minimum inhibitory concentration (MIC) was calculated.

Biofilm inhibition activity

The biofilm inhibition activity of nanomaterials (**1**, **2**, **1d**, **1e**, **2d**, and **2e**) was investigated against the bacteria *S. aureus* and *P. aeruginosa*. Different concentrations (5, 10, and 20 mg L^{-1}) of each nanomaterial (**1**, **2**, **1d**, **1e**, **2d**, or **2e**) were prepared in 24-well plates. Fresh suspensions of each bacterial species were inoculated into 24-well plates containing nutrient broth (NB) medium and incubated for 72 h at 37 °C to allow the cells to adhere to the surface. The biofilm-coated wells of the 24-well plate were meticulously cleaned twice using 200 μL of phosphate-buffered saline (PBS) and exposed to air for 30 min to dry out. To measure biofilm production, 200 μL of 1% aqueous crystal violet solution was applied to each plate well. The biofilm was left to stain for 60 min. The plates were cleaned with PBS to remove crystal violet. After the addition of ethanol, the absorbed crystal violet was recovered at room temperature after 15 min. The absorbance was measured at 595 nm using a spectrophotometer. The biofilm inhibition activity of nanostructures (**1**, **2**, **1d**, **1e**, **2d**, and **2e**) was calculated using eqn (3).

$$\text{Biofilm Inhibition}\,(\%) = \left(\frac{\text{Abs}_{\text{control}} - \text{Abs}_{\text{sample}}}{\text{Abs}_{\text{control}}}\right) \times 100 \quad (3)$$

Microbial cell viability inhibition without and with photodynamic therapy (PDT)

An *E. coli* strain (ATCC 25922) was employed as a "model" organism to examine the microbial cell viability inhibition of nanostructures (**1**, **2**, **1d**, **1e**, **2d**, and **2e**). *E. coli* was injected into NB, cultivated for 24 h at 37.5 °C, and agitated at 150

rpm. The mixture was centrifuged twice and cleaned with sterile distilled water. Each nanomaterial (**1**, **2**, **1d**, **1e**, **2d**, or **2e**) at various final concentrations (5, 10, and 20 mg L^{-1}) was applied to *E. coli* at 37 °C for 90 min. The mixtures were diluted, cultivated on nutrient agar medium, and allowed to incubate at 37 °C for 24 h. The same method was used to examine the effect of PDT on inhibition of microbial cell viability except that the compounds were exposed to LED light for 30 min before being added to *E. coli*-containing samples. A red–orange light-emitting diode with a wavelength of 632 ± 2 nm and energy of 12 J cm^{-2} was used as the light source. Colonies were tallied after incubation for 24 h. The *E. coli* viability inhibition activity of nanostructures (**1**, **2**, **1d**, **1e**, **2d**, and **2e**) was determined using eqn (4).

$$\text{Inhibition of cell viability}\,(\%) = (A_{\text{control}} - A_{\text{sample}}/A_{\text{control}}) \times 100 \quad (4)$$

The mixture without any nanostructures was applied as a control.

Results and discussion

Synthesis and characterization

Scheme 1 shows the synthetic procedure for compound (**a**). Due to the strong acidic nature of the ester group, the hydronium ion of diethyl 2-(3,4-dicyano-2,5-bis(hexyloxy)-6-(4-(trifluoromethoxy) phenoxy)phenyl) malonate was removed by the addition of potassium hydroxide, and the related potassium salt was obtained. The resultant salt and 2-chloro-*N*,*N*-dimethylethylamine were dissolved in sufficient acetonitrile and stirred for 72 h at 80 °C. The reaction of the compound with 2-chloro-*N*,*N*-dimethylethylamine resulted in the target phthalonitrile derivative (**a**). The product was characterized using spectroscopy (^{1}H NMR and FT-IR). All data were in accordance with the predicted structure.

The synthetic routes for macromolecules (**b** and **c**) and their quaternary derivatives (**d** and **e**) are depicted in Scheme 2. Macromolecules (**b** and **c**) were prepared by cyclotetramerization of compound **a** in the presence of the related metal cation through a one-step process. DBU was used as a catalyst to create a basic medium. The transesterification of the precursor resulted in the replacement of ethyl groups with pentyl groups during cyclotetramerization in *n*-pentanol.[42] These macromolecules (**b** and **c**) were treated with iodomethane to prepare their water-soluble derivatives (**d** and **e**). The resulting metal phthalocyanines were characterized using spectroscopy (UV–vis, FT-IR, and MALDI-TOF). Results confirmed the synthesis of designed structures. In the UV–vis spectra of compounds (**b–d**), characteristic bands were observed at ~380 nm (B-bands) and ~710 nm (Q-bands). The Q-bands of compounds (**b** and **c**) were single, whereas those of quaternary compounds (**d** and **e**) were split.[76] In the FT-IR spectra of compounds (**b** and **c**), the disappearance of nitrile bands at ~2200 cm^{-1} confirmed the complete cycloteramerization of phthalonitrile derivative (**a**).

The surface of gold nanoparticles (**1**) and silver nanoparticles (**2**) was functionalized non-covalently with each compound (**d** or **e**) and characterized using TEM and SEM. Gold nanostructures (**1**) were synthesized with an average size of 14.19 ± 2.13 nm, whereas silver nanoparticles (**2**) were obtained with an average size of 14.89 ± 2.84 nm. In a neutral medium, the metal nanoparticles carried a negative charge, while the phthalocyanines carried a positive charge owing to the basic nature of nitrogen.[77] As a result, a combination of electrostatic and π–π interactions between the negative citrate moieties on the metal nanoparticle surfaces and the positive functional groups of the phthalocyanine molecules controlled the interaction of the metal nanoparticles and the phthalocyanines. In addition, the van der Waals forces between the bases and metal nanoparticles, as well as coordination interactions between nitrogen atoms and metal atoms, contributed to the adsorption of phthalocyanines onto the metal nanoparticles surfaces.[78,79] Generally, the nanoparticles aggregated after surface modification with metal phthalocyanines. There was no significant increase in the size of the nanoparticles after modification (<1 nm). TEM images of unmodified metal nano-

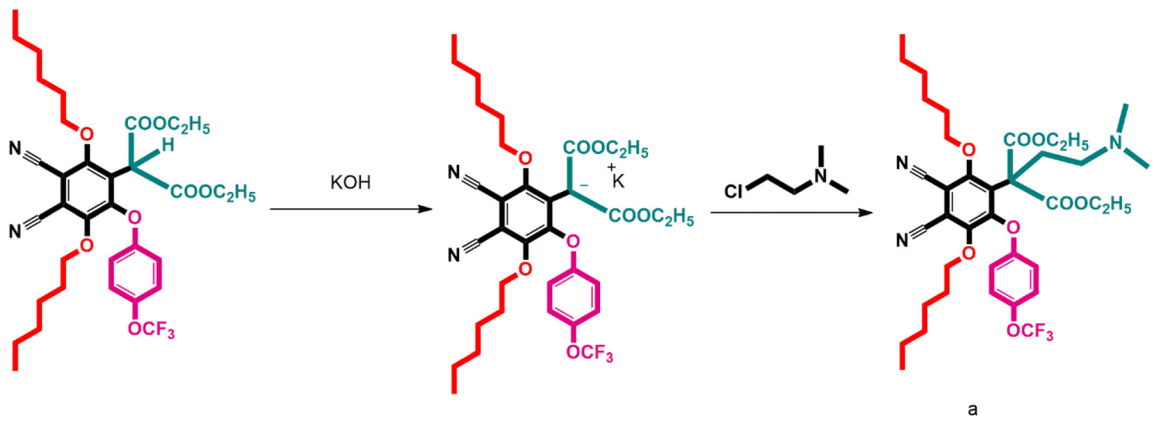

Scheme 1 Synthetic procedure for compound (**a**).

particles (**1** and **2**) and nanoconjugates (**1d** and **2e**) are demonstrated in Fig. 1. The changes detected in the SEM images of the nanoparticles before and after modification confirmed their surficial coverage with compound (**d** or **e**) (Fig. 2). Moreover, the FT-IR and UV–vis spectra of unmodified (**1** and **2**) and modified (**1d**, **1e**, **2d**, and **2e**) metal nanoparticles were studied. The characteristic peaks of the phthalocyanines appeared in the spectra of metal nanoparticles (**1** and **2**) in the most diluted sample. They confirmed the conjugation of the phthalocyanines on the surface of metal nanoparticles (refer to SI).

Antioxidant activity

Oxidants are responsible for apoptotic malfunction, inflammation, genetic change, and unchecked proliferation of cancer cells. These effects are exceedingly detrimental to living cells.[80] The DPPH free radical-scavenging assay is frequently used as a basic and highly effective screening method to evaluate the anti-radical activity of various substances. The DPPH free radical-scavenging activity of nanostructures (**1**, **2**, **1d**, **1e**, **2d** and **2e**) was examined in concentrations ranging from 6.25 to 100 mg L^{-1} (Fig. 3). The results were compared with data for two common standards (Trolox and ascorbic acid). As the concentration increased, the DPPH scavenging activity of nanostructures (**1**, **2**, **1d**, **1e**, **2d** and **2e**) enhanced from 29.63% to 49.82%, from 23.5% to 42.9%, from 40.88% to 62.77%, from 38.69% to 56.66%, from 37.23% to 54.97%, and from 30.80% to 45.73%, respectively. The antioxidant activity of nanostructures (**1**, **2**, **1d**, **1e**, **2d** and **2e**) diminished in the order **1d** > **1e** > **2d** > **1** > **2e** > **2**. The tested nanomaterials exhibited mod-

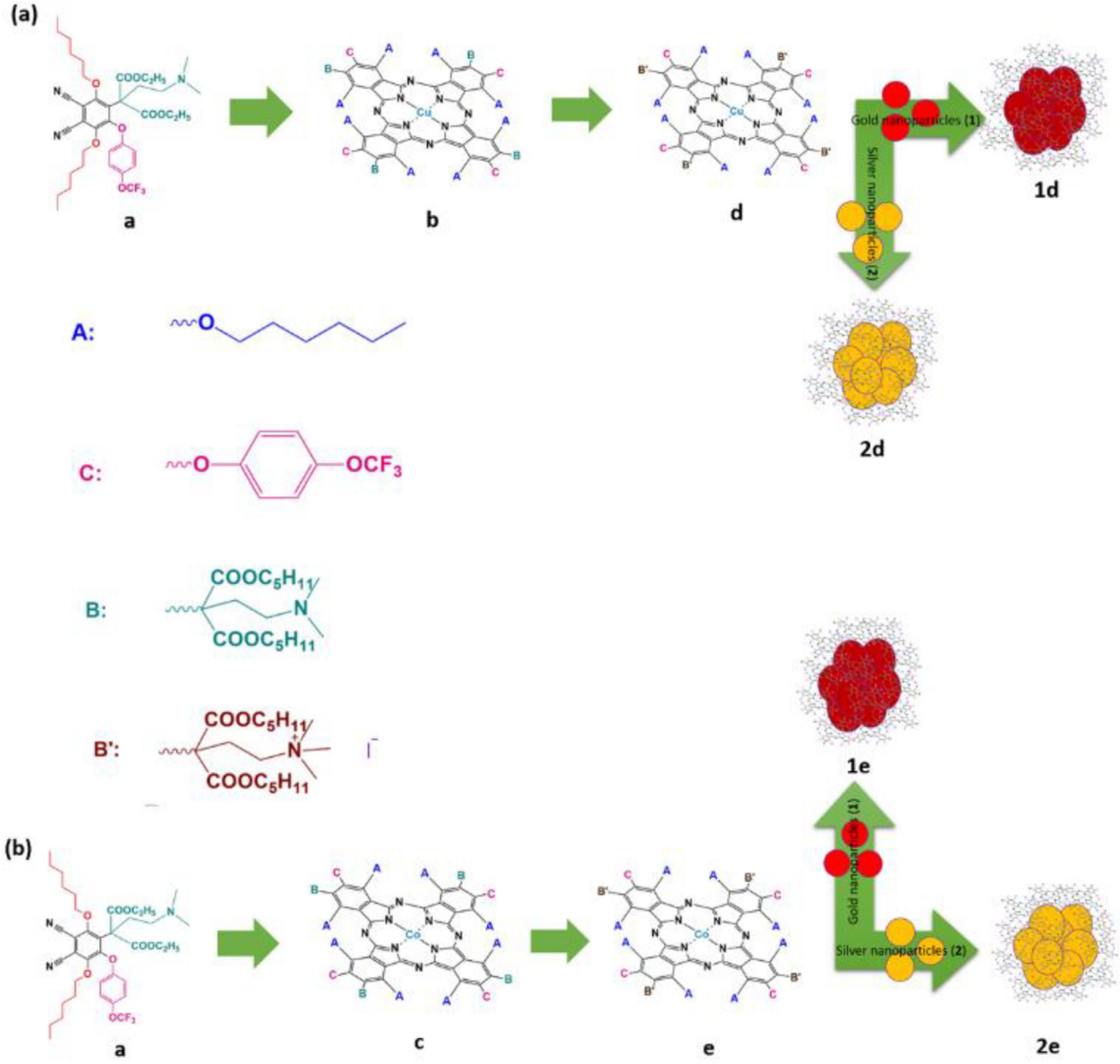

Scheme 2 Synthetic routes for (a) compounds (**b** and **d**) and nanoconjugates (**1d** and **2d**), (b) compounds (**c** and **e**) and nanoconjugates (**1e** and **2e**).

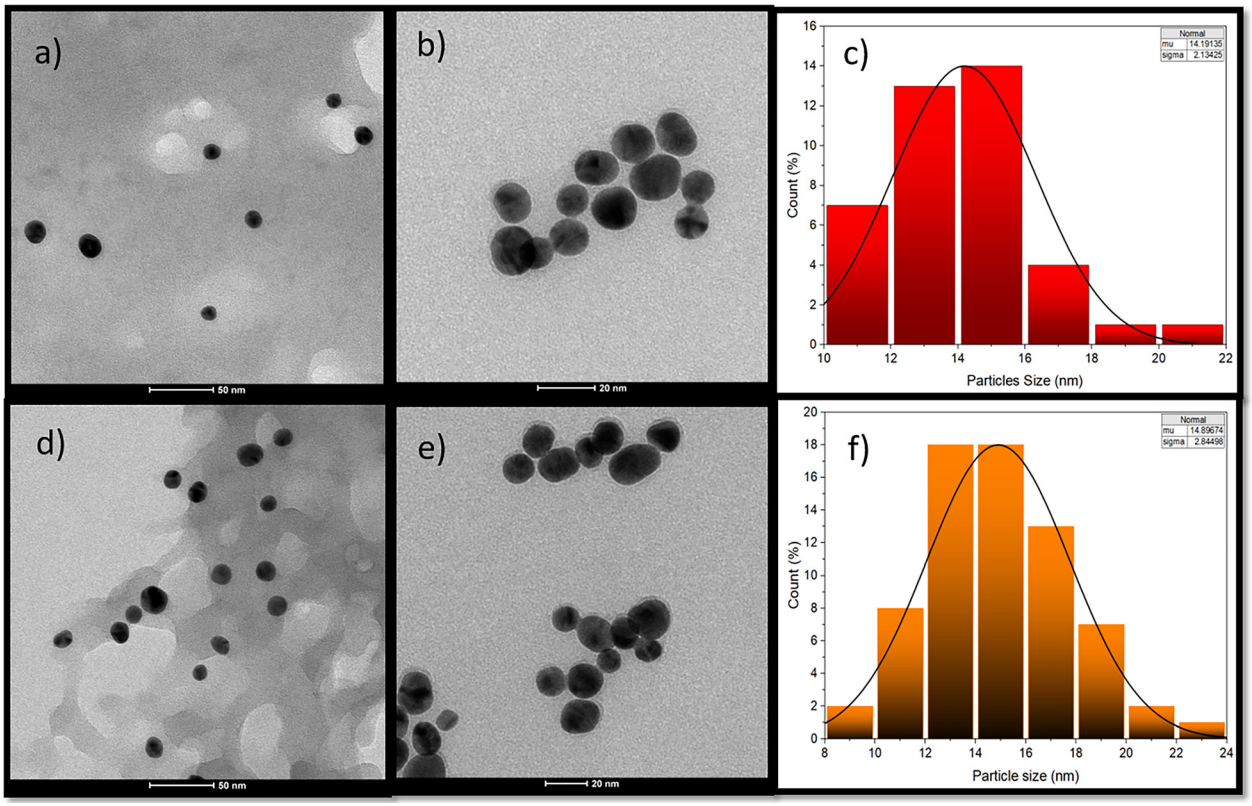

Fig. 1 TEM images of (a) unmodified gold nanoparticles (**1**) and (b) nanocojugate **1d**. (c) Histogram showing the size of gold nanoparticles. (d) TEM images of unmodified silver nanoparticles (**2**) and (e) nanocojugate **2e**. (f) Histogram showing the size of silver nanoparticles.

erate scavenging activity compared to the ascorbic acid and trolox. According to the literature, metallic nanostructures as well as metallo-phthalocyanine derivatives display significant antioxidant activity.[80–82] Compared with the literature, the surficial modification of nanoparticles (**1** and **2**) with the newly synthesized phthalocyanines (**d** and **e**) exhibited a synergistic enhancement of the individual antioxidant activities.

Antidiabetic activity

Diabetes mellitus is one of the most prevalent disorders affecting many people worldwide. Treatment usually focuses on enhancing the ability of cells to consume glucose or by decreasing carbohydrate absorption by inhibiting α-amylase enzyme.[83] The antidiabetic activity of nanostructures (**1**, **2**, **1d**, **1e**, **2d**, and **2e**) was investigated using an α-amylase activity assay (Fig. 4). The respective α-amylase inhibition activity of nanostructures (**1**, **2**, **1d**, **1e**, **2d**, and **2e**) was found to be 23.2, 45.3, 26.9, 31.8, 59.0, and 74.1% at 25 mg L^{-1}. As the concentration increased to 100 mg L^{-1}, the inhibition activity increased to 49.8, 81.1, 53.0, 58.5, 94.3 and 98.7%, respectively. Nanostructure (**2**) exhibited high inhibitory activity, but more effective inhibition was achieved by its conjugation with the newly synthesized metallo-phthalocyanines (**d** and **e**). These results are in accordance with the literature. Zubair *et al.* investigated the inhibitory activity of biogenic-synthesized silver nanoprisms. The resultant nanoprisms displayed 77.8% inhibitory activity at 100 mg L^{-1}.[84] Günsel *et al.* studied the antidiabetic activity of some new water-soluble tetra-substituted phthalocyanines. The phthalocyanines acted as a conventional glycosidase inhibitor.[85] In comparison with the studies mentioned above,[84,85] all the newly prepared nanostructures could be considered to be antidiabetic agents. In particular, nanomaterials **2**, **2d**, and **2e** significantly reduced α-amylase activity and had dose-dependent antidiabetic behaviour.

DNA cleavage activity

The DNA cleavage activity of nanostructures (**1**, **2**, **1d**, **1e**, **2d**, and **2e**) was examined using gel electrophoresis (a well-known method to study the especially separation of nucleic acids molecules). Accordingly, molecules moved at different rates on the gel and separated from each other at different rates after application of an electric field.[86] The DNA cleavage activity of nanostructures (**1**, **2**, **1d**, **1e**, **2d**, and **2e**) is demonstrated in Fig. 5 and 6. All the nanomaterials cleaved pBR322 plasmid DNA molecules. Use of 50 mg L^{-1} of nanomaterials (**1** and **2**) led to the conversion of the DNA from form I to form II, whereas these structures cleaved DNA molecules completely at 100 and 200 mg L^{-1}. Moreover, nanostructures (**1d**, **1e**, **2d**, and **2e**) displayed complete degradation of DNA molecules at all tested concentrations. After clinical research, nanomaterials (**1**, **2**, **1d**, **1e**, **2d**, and **2e**) could be considered to be alternative nanodrugs to prevent the proliferation of harmful organisms and cancer cells because they can cleave the genome.

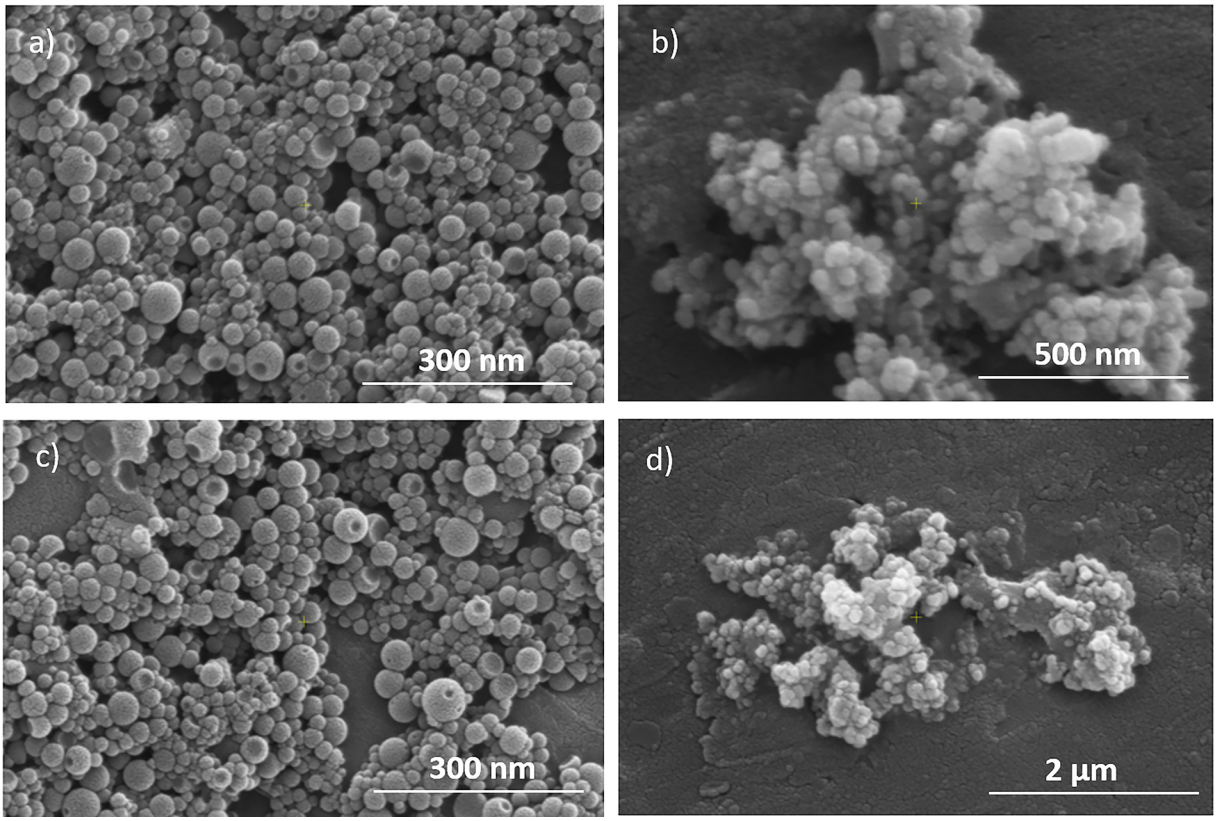

Fig. 2 SEM images of (a) unmodified gold nanoparticles, (b) nanocojugate **1d**, (c) unmodified silver nanoparticles and (d) nanocojugate **2e**, all at 25.00 kV.

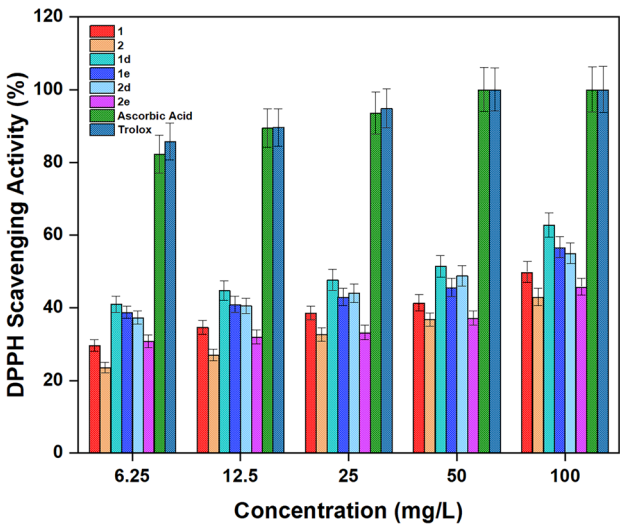

Fig. 3 DPPH-scavenging activity of gold nanoparticles (**1**), silver nanoparticles (**2**), QCuPc-gold nanoparticles (**1d**), QCoPc-gold nanoparticles (**1e**), QCuPc-silver nanoparticles (**2d**) and QCoPc-silver nanoparticles (**2e**).

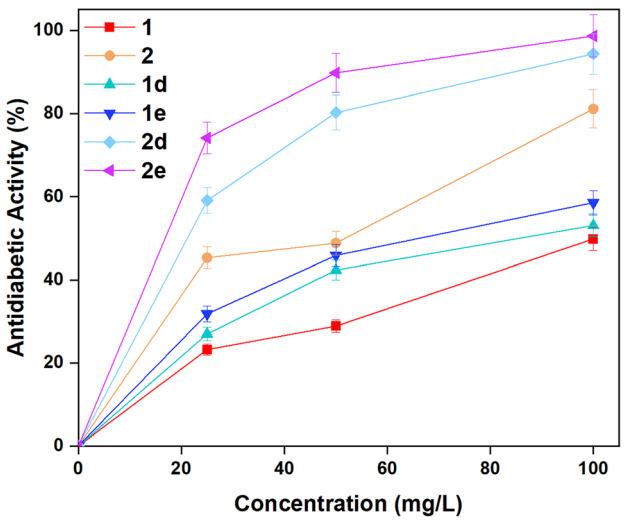

Fig. 4 Antidiabetic activity of gold nanoparticles (**1**), silver nanoparticles (**2**), QCuPc-gold nanoparticles (**1d**), QCoPc-gold nanoparticles (**1e**), QCuPc-silver nanoparticles (**2d**), and QCoPc-silver nanoparticles (**2e**).

Antimicrobial activity

The antimicrobial activity of nanostructures (**1**, **2**, **1d**, **1e**, **2d**, and **2e**) was tested against six bacterial and two fungal strains using a microdilution method. The MIC obtained for the antimicrobial activity of nanostructures (**1**, **2**, **1d**, **1e**, **2d**, and **2e**) ranged from 2 to 64 mg L^{-1} (Table 1). The antibacterial activity of nanomaterials (**1**, **2**, **1d**, **1e**, **2d**, and **2e**) was examined against *E. coli*, *P. aeruginosa*, *L. pneumophila* subsp. *pneumo-*

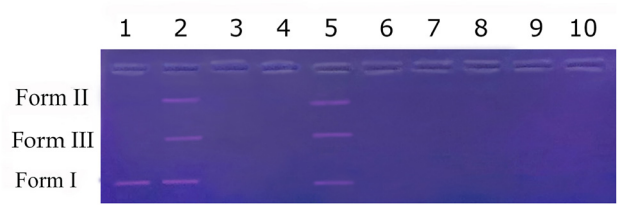

Fig. 5 DNA cleavage activity of nanostructures (**1**, **2**, and **1d**). Lane 1, pBR 322 DNA + DMSO. Lane 2, pBR 322 DNA + 50 mg L^{-1} of **1**. Lane 3, pBR 322 DNA + 100 mg L^{-1} of **1**. Lane 4, pBR 322 DNA + 200 mg L^{-1} of **1**. Lane 5, pBR 322 DNA + 50 mg L^{-1} of **2**. Lane 6, pBR 322 DNA + 100 mg L^{-1} of **2**. Lane 7, pBR 322 DNA + 200 mg L^{-1} of **2**. Lane 8, pBR 322 DNA + 50 mg L^{-1} of **1d**. Lane 9, pBR 322 DNA + 100 mg L^{-1} of **1d**. Lane 10, pBR 322 DNA + 200 mg L^{-1} of **1d**.

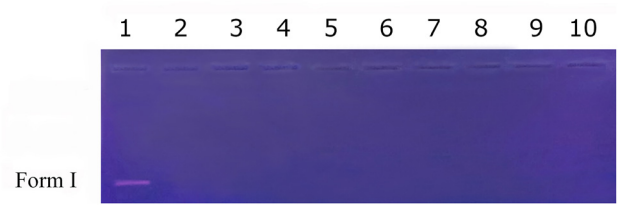

Fig. 6 DNA cleavage activity of nanostructures (**1e**, **2d**, and **2e**). Lane 1, pBR 322 DNA + DMSO. Lane 2, pBR 322 DNA + 50 mg L^{-1} of **1e**. Lane 3, pBR 322 DNA + 100 mg L^{-1} of **1e**. Lane 4, pBR 322 DNA + 200 mg L^{-1} of **1e**. Lane 5, pBR 322 DNA + 50 mg L^{-1} of **2d**. Lane 6, pBR 322 DNA + 100 mg L^{-1} of **2d**. Lane 7, pBR 322 DNA + 200 mg L^{-1} of **2d**. Lane 8, pBR 322 DNA + 50 mg L^{-1} of **2e**. Lane 9, pBR 322 DNA + 100 mg L^{-1} of **2e**. Lane 10, pBR 322 DNA + 200 mg L^{-1} of **2e**.

Table 1 MIC values of nanostructures **1**, **2**, **1d**, **1e**, **2d**, and **2e**

Microorganisms	1	2	1d	1e	2d	2e
E. coli	64	32	64	64	32	32
P. aeruginosa	64	32	64	32	32	64
L. pneumophila subsp. *pneumophila*	32	16	16	8	8	16
E. hirae	16	8	4	4	4	8
E. faecalis	16	4	4	2	2	8
S. aureus	64	32	32	64	32	32
C. parapsilosis	64	32	32	32	16	32
C. tropicalis	64	32	32	16	16	16

phila, *E. hirae*, *E. faecalis*, and *S. aureus* bacterial strains. All the nanostructures inhibited bacterial growth. In particular, nanomaterials (**1**, **2**, **1d**, **1e**, **2d**, and **2e**) demonstrated superior activity against *E. hirae* and *E. faecalis* strains in comparison with other bacteria. The respective MICs of nanostructures (**1**, **2**, **1d**, **1e**, **2d**, and **2e**) were 64, 32, 64, 64, 32, and 32 mg L^{-1} against *E. coli.* However, they displayed the highest inhibition activity against *E. faecalis*, with MICs ranging between 2 and 16 mg L^{-1}. Besides, the antifungal activity of nanomaterials (**1**, **2**, **1d**, **1e**, **2d**, and **2e**) was examined against *C. parapsilosis* and *C. tropicalis*. The MICs obtained were between 16 and 64 mg L^{-1} (Table 1). Nanoconjugate (**2d**) displayed the highest antifungal activity against both fungal strains (MIC = 16 mg L^{-1}). Many studies have reported the antimicrobial properties of individual metallic nanoparticles and phthalocyanines.[87–89] However, the antimicrobial activity of phthalocyanine-functionalized metallic nanostructures has not been reported. Our data indicate that phthalocyanine/metal nanoconjugates are promising candidates for further research and the development of antibacterial drugs.

Biofilm inhibition activity

Biofilms contribute to bacterial pathogenesis and increase the resistance of the pathogen to antibiotics by nearly 1000-fold.[90] The durability of biofilms is associated with the matrix, which is composed mostly of extracellular polymeric materials, proteins, lipids, and DNA molecules. Suitable conditions for bacteria to inhabit biofilm mode lead to strong resistance of bacteria to antibiotics. The biofilm inhibitory activity of nanomaterials (**1**, **2**, **1d**, **1e**, **2d**, and **2e**) was investigated against *S. aureus* and *P. aeruginosa* (Fig. 7 and 8). The respective biofilm inhibition activity of nanostructures (**1**, **2**, **1d**, **1e**, **2d**, and **2e**) was 79.5, 86.5, 87.3, 83.7, 89.1, and 85.7% against *S. aureus* at 20 mg L^{-1}. Moreover, nanomaterials (**1**, **2**, **1d**, **1e**, **2d**, and **2e**) inhibited 63.2, 80.7, 79.1, 74.3, 85.7, and 80.4% of *P. aeruginosa* biofilm formation at 20 mg L^{-1}, respectively. Nanoconjugate (**2d**) exhibited the highest biofilm inhibitory activity, whereas gold nanoparticles (**1**) displayed the lowest activity against both bacteria. Some studies have reported the individual biofilm inhibitory activity of metallic nanostructures and phthalocyanines.[91,92] Kumar *et al.* synthesized silver nanoparticles and studied their biofilm inhibitory properties. The inhibitory activity obtained was 67.5 and 67.1% against *S. aureus* and *B. subtilis*, respectively.[91] Çuhadar *et al.* prepared several metal phthalocyanines and examined their biofilm inhibition properties against *S. aureus* and *P. aeruginosa*. The highest inhibitory activity was 83.0 and 79.6% against *S. aureus* and *P. aeruginosa* for peripheral tetra-

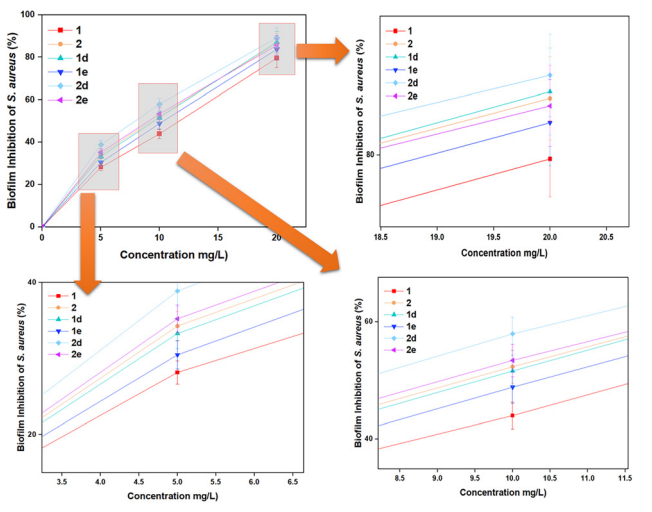

Fig. 7 Biofilm inhibitory activity of gold nanoparticles (**1**), silver nanoparticles (**2**), QCuPc-gold nanoparticles (**1d**), QCoPc-gold nanoparticles (**1e**), QCuPc-silver nanoparticles (**2d**), and QCoPc-silver nanoparticles (**2e**) against *S. aureus*.

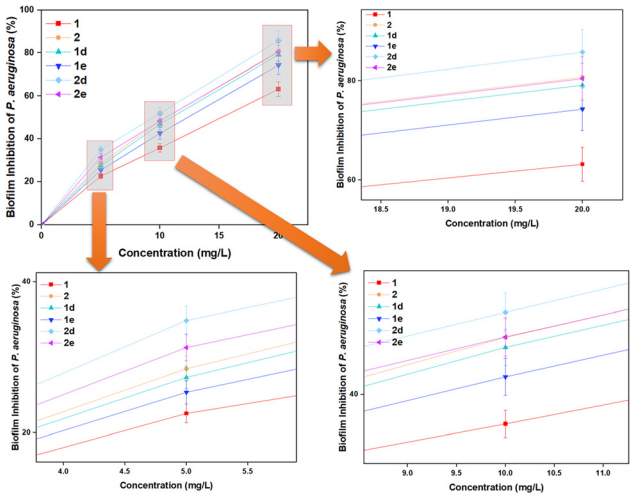

Fig. 8 Biofilm inhibition activity of gold nanoparticles (**1**), silver nanoparticles (**2**), QCuPc-gold nanoparticles (**1d**), QCoPc-gold nanoparticles (**1e**), QCuPc-silver nanoparticles (**2d**), and QCoPc-silver nanoparticles (**2e**) against *P. aeruginosa*.

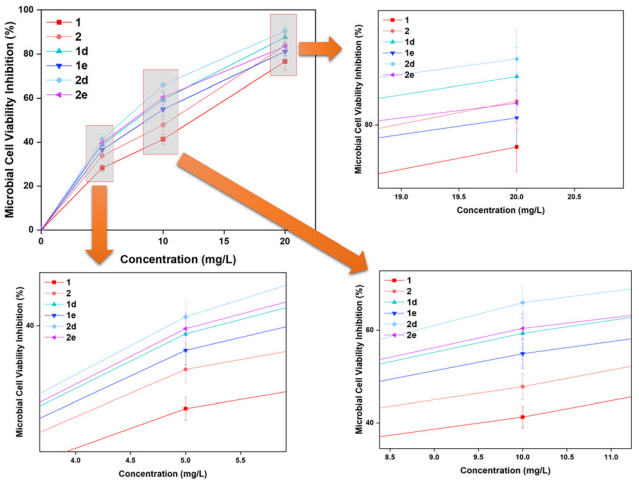

Fig. 9 Microbial cell viability inhibition activity of gold nanoparticles (**1**), silver nanoparticles (**2**), QCuPc-gold nanoparticles (**1d**), QCoPc-gold nanoparticles (**1e**), QCuPc-silver nanoparticles (**2d**), and QCoPc-silver nanoparticles (**2e**) without irradiation.

substituted Cu phthalocyanine, respectively.[92] The results obtained for nanomaterials (**1**, **2**, **1d**, **1e**, **2d**, and **2e**) are compatible with the literature; therefore, these structures, as potential biofilm inhibitory candidates, can form the basis for further research.

Microbial cell viability without and with PDT

E. coli is one of the most common disease-causing microorganisms worldwide. Humans and animals become ill or die from *E. coli* infection directly or indirectly. It serves an indicator microorganism for assessing microbial contamination in water and food (which are critical for human and animal health). For these reasons, it was also used in our study. The cell viability inhibitory activity of nanomaterials (**1**, **2**, **1d**, **1e**, **2d**, and **2e**) was investigated against *E. coli* at different concentrations (5, 10, and 20 mg L^{-1}) (Fig. 9). In general, an increase in the concentration of each nanostructure (**1**, **2**, **1d**, **1e**, **2d**, or **2e**) was followed by an enhancement in cell viability inhibitory activity (76.5% for (**1**), 83.8% for (**2**), 87.6% for (**1d**), 81.1% for (**1e**), 90.4% for (**2d**), and 83.4% % for (**2e**) at 20 mg L^{-1}). In contrast to the negative control, all nanomaterials displayed high inhibitory activity. Nanoparticles interact very well with bacteria owing to their high surface-to-area ratio, so they can neutralize the DNA replication activity of bacteria. Meanwhile, metal phthalocyanines can inhibit the cell viability of bacteria by generating ROS. Femi-Adepoju *et al.* reported the synthesis of silver nanoparticles using *Gleichenia pectinata* seed extracts.[93] The prepared nanoparticles exhibited good cell inhibitory properties. Farajzadeh *et al.* reported 100% microbial cell viability inhibitory activity for cobalt(II) and lutetium(III) phthalocyanines.[94]

Photoinactivating bacteria in the presence of a photosensitizer is known as "photodynamic antimicrobial chemotherapy" (PACT). In PACT, a photosensitizer is exposed to light at a certain wavelength. The interaction of the activated-photosensitizer with oxygen results in the production of some deadly ROS that in turn damage bacteria. The photosensitizing properties of phthalocyanines have attracted attention in antimicrobial research.[95,96] The PACT activity of nanostructures (**1**, **2**, **1d**, **1e**, **2d**, and **2e**) was investigated against *E. coli* at concentrations ranging from 5 to 20 mg L^{-1} (Fig. 10). Generally, the microbial cell viability inhibitory activity of nanostructures (**1**, **2**, **1d**, **1e**, **2d**, and **2e**) increased with irradiation. The respective microbial cell viability inhibitory activity of unmodified metallic nanoparticles (**1** and **2**) was 91.1% and 96.4%, whereas that of nanoconjugates (**1d**, **1e**, **2d**, and **2e**) was 100%, respectively.

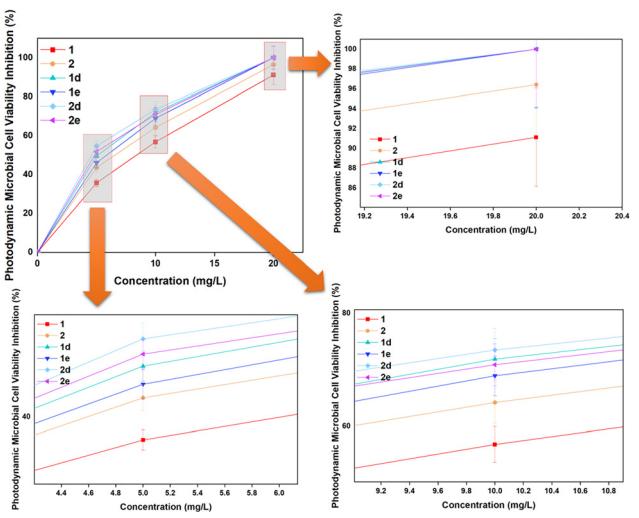

Fig. 10 Microbial cell viability inhibition activity of gold nanoparticles (**1**), silver nanoparticles (**2**), QCuPc-gold nanoparticles (**1d**), QCoPc-gold nanoparticles (**1e**), QCuPc-silver nanoparticles (**2d**), and QCoPc-silver nanoparticles (**2e**) with irradiation.

These data are in accordance with the literature and our previous studies.[97] As a result, all the nanostructures, especially nanoconjugates (**1d**, **1e**, **2d**, and **2e**), could be considered potential photosensitizers for PACT applications.

Conclusions

We report the design of new phthalocyanine-modified metal nanostructures exhibiting multidisciplinary biological features. The effect of the metal nature on the biological activities of unmodified and phthalocyanine-modified metallic nanoparticles was investigated, for the first time, in this study. A new tetra-substituted phthalonitrile derivative was synthesized and cyclotetramerized in the presence of suitable metal salts to prepare its copper(II) and cobalt(II) phthalocyanines. The water-soluble derivatives of the newly synthesized phthalocyanines were obtained *via* their reaction with iodomethane. The resultant quaternary macromolecules were used for surficial modification of two types of metal nanostructures (gold nanoparticles and silver nanoparticles), prepared as described in the literature with some modification. The antioxidant, antidiabetic, DNA cleavage, and antimicrobial activities of unmodified and modified metal nanoparticles were examined to study the effect of the modifying group and the type of metallic nanoparticles on biological properties. All modified nanomaterials, especially silver nanostructures, displayed effective DNA cleavage and antidiabetic activities. In addition, they exhibited moderate radical-scavenging activities at the studied concentrations. All nanostructures demonstrated significant antibacterial activity, especially against Gram-positive bacteria, and inhibited biofilm formation. Phthalocyanine-silver nanoconjugates displayed 100% cell viability inhibition activity against *E. coli* with irradiation. In our previous studies, the tested phthalocyanines were not water-soluble. However, placement on the surface of the nanomaterials improved their solubility in aqueous media. In the present study, the preparation of quaternary phthalocyanines positively affected the biological activities of the nanoconjugates owing to the refinement of modification and solubility. As a result, all nanoconjugates, especially modified silver nanoparticles, could be considered multidisciplinary agents for the development of novel medications and ongoing investigations.

Conflicts of interest

There are no conflicts of interest to declare.

Data availability

The data that support the findings of our study are available from the corresponding author upon reasonable request.

Supplementary information is available. See DOI: **https://doi.org/10.1039/d5dt01232e**.

Acknowledgements

This study was supported by Scientific and Technological Research Council of Turkey (TUBITAK; 222Z209). The authors thank TUBITAK for their support. Also, this work was supported financially by the Higher Education Council of Türkiye. The authors appreciate the funding provided by Research Fund of the Istanbul Technical University (ADEP Project Number: TGA-2024-45319).

References

1 I. Ojima, *J. Org. Chem.*, 2013, **78**(13), 6358.
2 K. Müller, C. Faeh and F. Diederich, *Science*, 2007, **317**, 1881.
3 J. Wang, M. Sánchez-Roselló, J. L. Aceña, C. del Pozo, A. E. Sorochinsky, S. Fustero, V. A. Soloshonok and H. Liu, *Chem. Rev.*, 2014, **114**, 2432.
4 E. P. Gillis, K. J. Eastman, M. D. Hill, D. J. Donnelly and N. A. Meanwell, *J. Med. Chem.*, 2015, **58**, 8315.
5 A. Strunecká, J. Patočk and P. Connett, *J. Appl. Biomed.*, 2004, **2**, 141.
6 M. Kasprzak, M. Rudzinska, D. Kmiecik, R. Przybylski and A. Olejnik, *Food Chem. Toxicol.*, 2020, **136**, 111074.
7 M. Brigante, C. Emmelin, L. Previtera, R. Baudot and J. M. Chovelon, *J. Agric. Food Chem.*, 2005, **53**(13), 5347.
8 S. Q. Du, Q. L. Yuan, X. P. Hu, W. Fu, Q. Xu, Z. Y. Wei, J. Z. Xu, X. S. Shao and X. H. Qian, *J. Agric. Food Chem.*, 2021, **69**(51), 15521.
9 Q. L. Yuan, Y. C. Zhang, S. Q. Du, W. Fu, Z. P. Xu, J. G. Cheng, Z. Li and X. S. Shao, *J. Heterocycl. Chem.*, 2023, **60**(5), 781.
10 M. Ulgen and N. Sevinc, *Curr. Drug Metab.*, 2017, **18**(4), 291.
11 S. S. Ozbek, S. T. Tuncel, S. E. Gunal and I. Dogan, *Chirality*, 2025, **37**(2), e70013.
12 G. P. Coskun, Y. Ozhan, V. Dobričić, J. Bošković, R. Reis, H. Sipahi, Z. Sahin and S. Demirayak, *Pharmaceutics*, 2023, **15**, 1441.
13 L. Zhao, L. Zhu and H. K. Lee, *J. Chromatogr. A*, 2002, **963**(1–2), 239.
14 H. M. Pinheiro, E. Touraud and O. Thomas, *Dyes Pigm.*, 2004, **61**, 121.
15 L. Muller, E. Fattore and E. Benfenati, *J. Chromatogr. A*, 1997, **791**, 221.
16 T. S. Balaban, H. Tamiaki and A. R. Holzwarth, Chlorins Programmed for Self-Assembly, in *Supermolecular Dye Chemistry, Topics in Current Chemistry*, ed. F. Würthner, Springer, Berlin, Heidelberg, 2005, vol. 258.
17 C. C. Leznoff and A. B. P. Lever, *Phthalocyanines Properties and Applications*, VCH, New York, 1989, 1993 n 1996, vols. 1–4.
18 Ö. Bekaroğlu, *Appl. Organomet. Chem.*, 1996, **10**(8), 605.
19 M. B. Koçak, *J. Porphyrins Phthalocyanines*, 2000, **4**, 742.
20 Z. A. Bayır, *Dyes Pigm.*, 2005, **65**(3), 235.

21 T. Stuchinskaya, M. Moreno, M. J. Cook, D. R. Edwards and D. A. Russell, *Photochem. Photobiol. Sci.*, 2011, **10**, 822.
22 Ş. Özçelik, A. Koca and A. Gül, *Polyhedron*, 2012, **42**(1), 227.
23 C. Uslan, K. T. Oppelt, L. M. Reith, B. Ş. Sesalan and G. Knör, *Chem. Commun.*, 2013, **49**, 8108.
24 M. Wierzchowski, L. Sobotta, P. Skupin-Mrugalska, J. Kruk, W. Jusiak, M. Yee, K. Konopka, N. Düzgüneş, E. Tykarska, M. Gdaniec, J. Mielcarek and T. Goslinski, *J. Inorg. Biochem.*, 2013, **127**, 62.
25 H. Y. Yenilmez, A. M. Sevim and Z. A. Bayır, *Synth. Met.*, 2013, **176**, 11.
26 N. Hamdi, R. Medyouni, A. S. Al-Ayed, L. Mansour and A. Romerosa, *J. Heterocycl. Chem.*, 2017, **54**, 2342.
27 A. Kalkan, A. Koca and Z. A. Bayır, *Polyhedron*, 2004, **23**(18), 3155.
28 İ. Özçeşmeci, M. Özçeşmeci, A. Gül and E. Hamuryudan, *Synth. Met.*, 2016, **222**, 344.
29 E. Kumral, H. Y. Yenilmez, S. Albayrak, A. N. Şahin, A. Altındal and Z. A. Bayır, *Dalton Trans.*, 2020, **49**, 9385.
30 N. Farajzadeh, H. P. Karaoğlu, M. Akin, N. Saki and M. B. Koçak, Antimicrobial and antioxidant properties of novel octa-substituted phthalocyanines bearing (trifloromethoxy)phenoxy groups on peripheral positions, in Porphyrin Science by Women, *Biomedical*, 2021, **1**, 226.
31 N. Farajzadeh, Ç. Çelik, G. Y. Atmaca, S. Özdemir, S. Gonca, A. Erdoğmuş and M. B. Koçak, *Dalton Trans.*, 2022, **51**, 478.
32 Ç. Çelik, N. Farajzadeh, M. Akın, G. Y. Atmaca, Ö. Sağlam, N. Şaki, A. Erdoğmuş and M. B. Koçak, *Dalton Trans.*, 2021, **50**, 2736.
33 E. Boisselier and D. Astruc, *Chem. Soc. Rev.*, 2009, **38**, 1759.
34 D. F. Moyano and V. M. Rotello, *Langmuir*, 2011, **27**, 10376.
35 M. C. Heffern, N. Yamamoto, R. J. Holbrook, A. L. Eckermann and T. J. Meade, *Curr. Opin. Chem. Biol.*, 2013, **17**(2), 189.
36 S. Krupanidhi, A. Sreekumar and C. B. Sanjeevi, *Indian J. Med. Res.*, 2008, **128**(4), 448.
37 S. Albayrak, N. Farajzadeh, H. Y. Yenilmez, S. Özdemir, S. Gonca and Z. A. Bayır, *Chem. Biodivers.*, 2023, **20**(7), e202300389.
38 Ö. İ. Öney, H. Y. Yenilmez, D. Bahar, N. F. Öztürk and Z. A. Bayır, *Dalton Trans.*, 2023, **52**, 13119.
39 N. Farajzadeh, H. Y. Yenilmez, D. Bahar, N. G. Kuşçulu, E. K. Selvi and Z. A. Bayır, *Dalton Trans.*, 2023, **5**, 94144.
40 N. Farajzadeh, J. Aftab, H. Y. Yenilmez, S. Özdemir, S. Gonca and Z. A. Bayır, *New J. Chem.*, 2022, **46**, 5374.
41 J. Aftab, N. Farajzadeh, H. Y. Yenilmez, S. Özdemir, S. Gonca and Z. A. Bayır, *Dalton Trans.*, 2022, **51**, 4466.
42 N. F. Öztürk, S. Özdemir, G. Giray, J. Aftab and Z. A. Bayır, *ChemistrySelect*, 2024, **9**(1), e202303907.
43 N. F. Öztürk, S. Özdemir, M. S. Yalçın, G. Tollu, Z. A. Bayır and M. B. Koçak, *ACS Appl. Bio Mater.*, 2024, **7**(5), 3215.
44 B. Bhushan, Introduction to Nanotechnology, in *Springer Handbook of Nanotechnology*, Springer, Berlin, Heidelberg, 2017.
45 T. Lakshmipriya and C. B. S. Gopinath, Introduction to nanoparticles and analytical devices, in *Nanoparticles in Analytical and Medical Devices*, Elsevier, Amsterdam, Netherlands, 2021, vol. 1.
46 G. Marcelo, E. Kaplan, M. P. Tarazona and F. Mendicuti, *Colloids Surf., B*, 2015, **128**, 237.
47 K. Kusat and S. Akgöl, *Nanobiosensors: Usability of Imprinted Nanopolymers, Molecular Imprinting for Nanosensors and Other Sensing Applications*, Elsevier, Amsterdam, Netherlands, 2021, ch. 7, p. 163..
48 C. Sun, F. Li, H. An, Z. Li, A. M. Bond and J. Zhang, *Electrochim. Acta*, 2018, **269**, 733.
49 S. Lin, Y. Cheng, J. Liu and M. R. Wiesner, *Langmuir*, 2012, **28**, 4178.
50 G. Rath, T. Hussain, G. Chauhan, T. Garg and A. K. Goyal, *J. Drug Targeting*, 2016, **24**(6), 520.
51 G. Naja, P. Bouvrette, S. Hrapovic and J. H. T. Luong, *Analyst*, 2007, **132**, 679.
52 P. Prasher, M. Sharma, H. Mudila, G. Gupta, A. K. Sharma, D. Kumar, H. A. Bakshi, P. Negi, D. N. Kapoor, D. K. Chellappan, M. M. Tambuwala and K. Dua, *Colloid Interface Sci. Commun.*, 2020, **35**, 100244.
53 A. A. Rakhmetova, T. P. Alekseeva, O. A. Bogoslovskaya, I. O. Leipunskii, I. P. Ol'khovskaya, A. N. Zhigach and N. N. Glushchenko, *Nanotechnol. Russ.*, 2010, **5**, 271.
54 S. A. Khan, S. Shahid and F. Ijaz, *Green Synthesis of Copper oxide Nanoparticles & Biomedical Application*, Lap Lambert Academic Publishing, 2017.
55 Y. P. Jia, B. Y. Ma, X. W. Wei and Z. Y. Qian, *Chin. Chem. Lett.*, 2017, **28**(4), 691.
56 S. Mukherjee, S. Sau, D. Madhuri, V. S. Bollu, K. Madhusudana, B. Sreedhar, R. Banerjee and C. R. Patra, *J. Biomed. Nanotechnol.*, 2016, **12**(1), 165.
57 M. Negahdary, R. Chelongar, S. K. Zadeh and M. Ajdary, *Adv. Biomed. Res.*, 2015, **4**(1), 69.
58 B. C. Nelson, E. J. Petersen, B. J. Marquis, D. H. Atha, J. T. Elliott, D. Cleveland, S. S. Watson, I. H. Tseng, A. Dillon, M. Theodore and J. Jackman, *Nanotoxicology*, 2013, **7**(1), 21.
59 J. H. Sung, J. H. Ji, J. D. Park, M. Y. Song, K. S. Song, H. R. Ryu, J. U. Yoon, K. S. Jeon, B. S. Han, Y. H. Chung, H. K. Chang, J. H. Lee, D. W. Kim, B. J. Kelman and I. J. Yu, *Part. Fibre Toxicol.*, 2011, **8**(1), 16.
60 S. J. Cameron, F. Hosseinian and W. G. Willmore, *Int. J. Mol. Sci.*, 2018, **19**, 2030.
61 L. Q. Chen, L. Fang, J. Ling, C. Z. Ding, B. Kang and C. Z. Huang, *Chem. Res. Toxicol.*, 2015, **28**(3), 501.
62 Z. Guo, G. Zeng, K. Cui and A. Chen, *Environ. Chem. Lett.*, 2018, **17**(1), 319.
63 J. Pulit-Prociak, K. Stokłosa and M. Banach, *Environ. Chem. Lett.*, 2014, **13**(1), 59.
64 M. R. Mulenos, J. Liu, H. Lujan, B. Guo, E. Lichtfouse, V. K. Sharma and C. M. Sayes, *Environ. Chem. Lett.*, 2020, **18**, 1319.
65 C. Woese, O. Kandler and M. Wheelis, *Proc. Natl. Acad. Sci. U. S. A.*, 1990, **87**, 4576.
66 P. Hugenholtz, B. M. Goebel and N. R. Pace, *J. Bacteriol.*, 1998, **80**, 4765.

67 (*a*) J. G. Caporaso, C. L. Lauber, W. A. Walters, D. Berg-Lyons, J. Huntley, N. Fierer, S. M. Owens, J. Betley, L. Fraser, M. Bauer, N. Gormley, J. A. Gilbert, G. Smith and R. Knight, *ISME J.*, 2012, **6**(8), 1621; (*b*) H. Han, H. Yılmaz and I. Gulcin, *Rec. Nat. Prod.*, 2018, **12**(4), 397.
68 J. Szymczak, L. Sobotta, J. Dlugaszewska, M. Kryjewski and J. Mielcarek, *Dyes Pigm.*, 2021, **193**, 109410.
69 N. N. Saki, M. Akin, A. Atsay, H. R. P. Karaoglu and M. B. Kocak, *Inorg. Chem. Commun.*, 2018, **95**, 122.
70 L. Chetry, P. P. Sarma and P. K. Baruah, *Colloids Surf., A*, 2025, **720**, 137156.
71 N. F. Öztürk, H. Z. Uzunmehmetoglu, H. Y. Yenilmez, S. Özdemir, A. Dundar and Z. A. Bayır, *ACS Omega*, 2025, **10**(27), 28709.
72 M. Rezai, Ç. Bayrak, P. Taslimi, I. Gulcin and A. Menzek, *Turk. J. Chem.*, 2018, **42**(3), 808.
73 S. Cakmakci, E. F. Topdaş, P. Kalın, H. Han, P. Şekerci, L. P. Kose and I. Gulcin, *Int. J. Food Sci. Technol.*, 2015, **50**(2), 472.
74 H. A. Dinçer, E. Gonca and A. Gül, *Dyes Pigm.*, 2008, **79**, 166.
75 L. Mulfinger, D. S. Solomon, M. Bahadory, A. V. Jeyarajasingam, S. A. Rutkowsky and C. Boritz, *J. Chem. Educ.*, 2007, **84**, 322.
76 S. Tuncel, F. Dumoulin, J. Gailer, M. Sooriyaarachchi, D. Atilla, M. Durmuş, D. Bouchu, H. Savoie, R. W. Boyle and V. Ahsen, *Dalton Trans.*, 2011, **40**, 4067.
77 L. Hou, W. Li, Z. Wu, Q. Wei, H. Yang, Y. Jiang, T. Wang, Y. Wang and Q. He, *Sep. Purif. Technol.*, 2022, **290**, 120858.
78 H. Li and L. Rothberg, *Proc. Natl. Acad. Sci. U. S. A.*, 2004, **101**(39), 14036–14039.
79 L. Wang, X. Liu, X. Hu, S. Song and C. Fan, *Chem. Commun.*, 2006, 3780.
80 C. Kamaraj, C. Ragavendran, K. Manimaran, S. Sarvesh, A. R. M. Towfiqul Islam and G. Malafaia, *Sci. Total Environ.*, 2023, **861**, 160575.
81 A. Aygün, S. Özdemir, M. Gülcan, M. S. Yalçın, M. Uçar and F. Şen, *Int. J. Environ. Sci. Technol.*, 2022, **19**, 2781.
82 B. Barut and U. Demirbaş, *J. Organomet. Chem.*, 2020, **923**, 121423.
83 V. Haritha, S. Gowri, B. Janarthanan, Md. Faiyazuddin, C. Karthikeyan and S. Sharmila, *Inorg. Chem. Commun.*, 2022, **144**, 109930.
84 M. Zubair, M. Azeem, R. Mumtaz, M. Younas, M. Adrees, E. Zubair, A. Khalid, F. Hafeez, M. Rizwan and S. Ali, *Environ. Pollut.*, 2022, **304**, 119249.
85 A. Günsel, G. Y. Atmaca, P. Taslimi, A. T. Bilgiçli, İ. Gülçin, A. Erdoğmuş and M. N. Yarasir, *J. Photochem. Photobiol., A*, 2020, **396**, 112511.
86 N. V. Kulkarni, A. Kamath, S. Budagumpi and V. K. Revankar, *J. Mol. Struct.*, 2011, **1006**(1–3), 580.
87 A. V. A. Mariadoss, V. Ramachandran, V. Shalini, B. Agilan, J. H. Franklin, K. Sanjay, Y. G. Alaa, T. M. Al-Antary and D. Ernest, *Microb. Pathog.*, 2019, **135**, 103609.
88 A. Aghajanyan, L. Gabrielyan, R. Schubert and A. Trchounian, *AMB Express*, 2020, **10**, 66.
89 P.-P. Fan, S.-L. Li, B.-Y. Zheng, B.-D. Zheng, L.-L. Lv, M.-R. Ke and J.-D. Huang, *Dyes Pigm.*, 2023, **212**, 111122.
90 C. W. Hall and T. F. Mah, *FEMS Microbiol. Rev.*, 2017, **41**, 276.
91 S. Kumar, H. M. Khan, M. A. Khan, M. Jalal, S. Ahamad, M. Shahid, F. M. Husain, M. Arshad and M. Adil, *J. King Saud Univ., Sci.*, 2023, **35**(8), 102904.
92 B. Çuhadar, A. K. Burat, G. Giray and S. Özdemir, *Polyhedron*, 2023, **244**, 116593.
93 A. G. Femi-Adepoju, A. O. Dada, K. O. Otun, A. O. Adepoju and O. P. Fatoba, *Heliyon*, 2019, **5**(4), e01543.
94 N. Farajzadeh, S. Özdemir, G. Tollu, Z. A. Bayır and M. B. Koçak, *J. Inorg. Biochem.*, 2022, **234**, 111888.
95 Y. Gao, B. Mai, A. Wang, M. Li, X. Wang, K. Zhang, Q. Liu, S. Wei and P. Wang, *Photodiagn. Photodyn. Ther.*, 2018, **21**, 316.
96 M. Li, B. Mai, A. Wang, Y. Gao, X. Wang, X. Liu, S. Song, Q. Liu, S. Wei and P. Wang, *RSC Adv.*, 2017, **7**, 40734.
97 N. Farajzadeh, Ç. Çelik, S. Özdemir and S. Gonca, *New J. Chem.*, 2022, **46**(15), 7177.